BUTTERWORTH HEINEMANN

*Polymer* Vol. 36 No. 18, pp. 3485–3492, 1995

0032-3861/95/$10.00+0.00

# Yielding and hysteresis of polymer fibres

**M. G. Northolt*, J. J. M. Baltussen and B. Schaffers-Korff**
*Akzo Nobel Central Research, PO Box 9300, 6800 SB Arnhem, The Netherlands*
*(Received 13 December 1994)*

The yielding phenomenon in the tensile curves of polymer fibres is explained by the onset of a sequential and plastic orientation mechanism of the chains brought about by the resolved shear stress. The proposed simple theory shows that the yield strain in tension and compression varies from 0.5% for highly oriented fibres to about 2.2% for randomly oriented specimens, and that this range is the same for aliphatic polyamide, poly(ethylene terephthalate), cellulose II and poly(*p*-phenylene terephthalamide) fibres. In addition, the yielding mechanism explains the difference between the first loading tensile curve and the hysteresis curves of these fibres.

**(Keywords: tensile deformation; compression; yielding)**

## INTRODUCTION

At temperatures below the glass transition, fibres of aliphatic polyamides, poly(ethylene terephthalate) (PET), cellulose II and poly(*p*-phenylene terephthalamide) (PpPTA) have essentially the same kind of tensile curve. As shown in *Figures 1* and *2*, these curves consist of a nearly straight part up to the yield strain between 0.5 and 2.0%, a short yield range characterized by a decrease of the slope, followed by a more or less concave section almost up to fracture. These three stages are more pronounced in fibres with medium and low orientation, such as polyamide 66 (PA 66), PET and cellulose II, than in highly oriented fibres, such as Twaron® (PpPTA) and cellulose II EHM. The curves of some of the fibres with low and medium orientation often show, in addition, a small convex or even flat part just before fracture. This similarity in shape extending over a considerable part of the tensile curve indicates that the tensile behaviour of these fibres is governed by the same deformation mechanism. Well oriented fibres yield in the range of 0.5 to 1.0% strain, whereas isotropic samples show a yield strain at about 2.2%. Unloading of the fibre after the first extension up to a strain larger than the yield strain results in a small but permanent extension of the fibre. As shown in *Figures 1* and *2*, it is remarkable that there is little variation in the yield strain, $\epsilon_y$, for fibres made of different kinds of polymer. It is this particular aspect that is explained by the simple theory presented in this paper.

A modified series model has been proposed for the elastic extension of oriented and (semi)crystalline fibres[1–3]. As will be shown in this study, the series model implies that the fibre extension is governed by a sequential orientation mechanism. The model also indicates the importance of the initial orientation distribution of the chain axes for the deformation of the fibre. Fibres obtained by melt spinning and hot drawing, such as PET fibres, as well as those made by a conventional wet spinning process, such as viscose rayon, have a distribution resembling the affine distribution[4–6]. This distribution is obtained by the affine deformation of an isotropic sample, which transforms an angle $\phi_0$ to $\phi$ according to $\tan\phi = \lambda^{(-3/2)}\tan\phi_0$ at a draw ratio of $\lambda$, resulting in the distribution:

$$\rho(\phi) = \frac{1}{4\pi}\frac{\lambda^3}{(\cos^2\phi + \lambda^3\sin^2\phi)^{3/2}} \qquad (1)$$

where $\phi$ is the angle of the chain axis relative to the fibre axis.

High modulus fibres, such as PpPTA, polybenzoxazole (PBO) and polybenzothiazole (PBT), are made by spinning lyotropic solutions[3]. It has been shown that in this process the director field of the domains in the solution is also deformed according to the affine deformation scheme. However, for high draw ratios the orientation distribution in the fibre is almost completely determined by the chain alignment within the individual domains, which is governed by the Maier–Saupe mean-field potential yielding a Gaussian-shaped distribution[7].

The proposed yielding model is based on the assumption of a shear yield stress, $\tau_y$, which is supposed to be a small fraction of the modulus for shear between the chains. The model provides an equation for the yield strain as a function of the orientation in the fibre and, together with the sequential orientation process, it also explains the difference between the first loading curve and the repeated loading or hysteresis curves of semicrystalline and wholly paracrystalline polymer fibres[8].

## THEORY

First, a brief recapitulation of the series model for a polymer fibre is presented[1–3]. The fibre is considered as being built up of a parallel array of identical fibrils which are subjected to a uniform stress along the fibre axis. Each fibril consists of a series of oblong domains arranged end to end. In a domain the chains run parallel

* To whom correspondence should be addressed

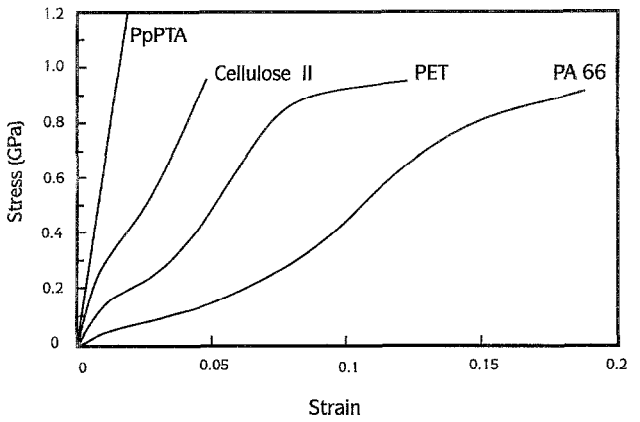


**Figure 1** Filament tensile curves of PA 66, PET, cellulose II and PpPTA fibres measured with a test length of 100 mm and a strain rate of 10% $min^{-1}$

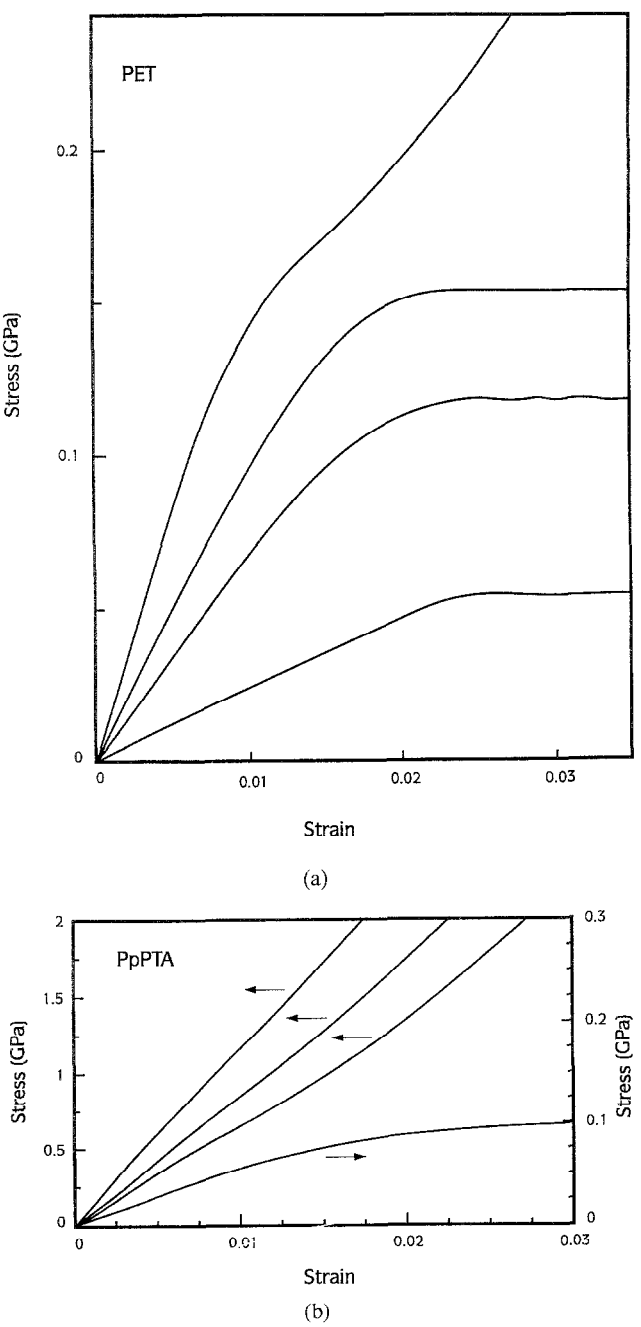


**Figure 2** Initial part of the filament tensile curves of (a) PET fibres and (b) PpPTA fibres with different degrees of orientation

to the symmetry axis which makes an angle $\phi$ with the fibre axis. All domains in a fibril are assumed to be isotropic transverse to the symmetry axis and to have identical mechanical properties. The orientation of the symmetry axes follows a distribution $\rho(\phi)$ measured along the meridian. Owing to the axial symmetry of the fibre, the function $N(\phi) = \rho(\phi)\sin\phi$ represents the fraction of domains with angle $\phi$ in the fibre. *Figure 3* shows $\rho(\phi)$ and $N(\phi)$ for a Gaussian and an affine distribution with the same value for the orientation parameter. The difference between the two distributions is particularly noticeable in the tails.

In the modified series model, the mechanical properties of a domain pertaining to the elastic extension of the fibril are the chain modulus, $e_c$, and the modulus for shear between the chains, $g$. This single shear modulus is an approximation since in many polymer fibres there is no isotropy in a plane transverse to the chain axis owing to the different kinds of intermolecular interactions resulting in triclinic, monoclinic or orthorhombic symmetry of the chain packing. According to this series model, the tensile modulus of the fibre is given by:

$$\frac{1}{E} = \frac{1}{e_c} + \frac{\langle \sin^2 \phi_0 \rangle_E}{2g} \tag{2}$$

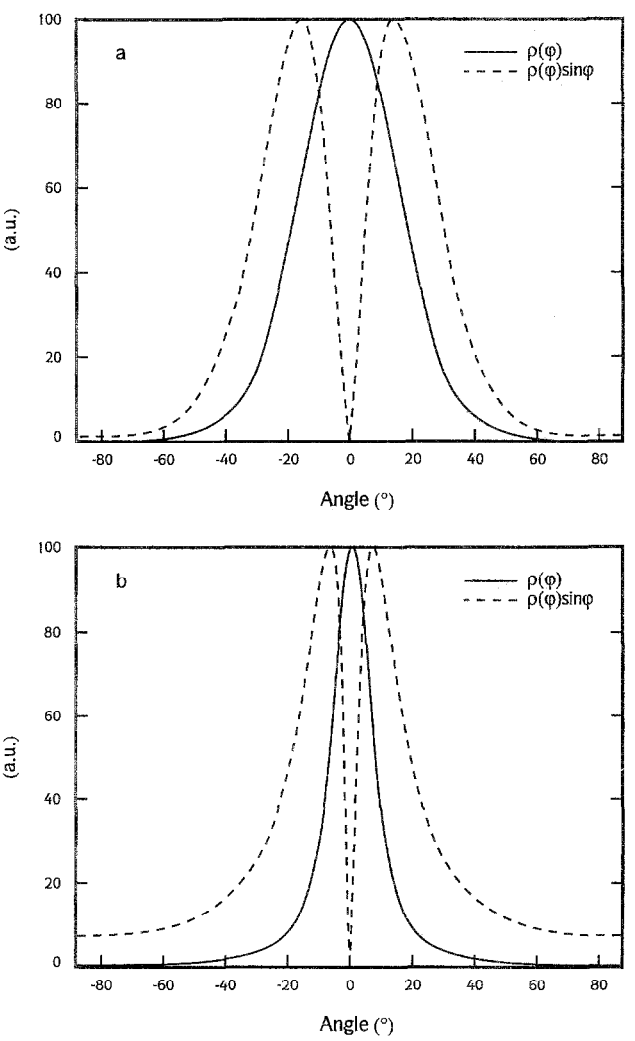


**Figure 3** (a) The Gaussian distribution, $\rho(\phi) = \exp(-p\sin^2\phi)$; (b) the affine distribution, $\rho(\phi) = (\lambda^3/4\pi)(\cos^2\phi + \lambda^3\sin^2\phi)^{(-3/2)}$. For both distributions, $\langle \sin^2\phi \rangle_E = 0.1471$ and $N(\phi) = \rho(\phi)\sin\phi$

where $\langle \sin^2 \phi_0 \rangle_E$ is the second moment of the chain or domain orientation distribution $\rho(\phi)$ before loading of the fibre and is defined as:

$$\langle \sin^2 \phi \rangle_E = \frac{\int_0^{\pi/2} \rho(\phi) \cos \phi \sin^3 \phi \, d\phi}{\int_0^{\pi/2} \rho(\phi) \cos \phi \sin \phi \, d\phi} \quad (3)$$

We will call $\langle \sin^2 \phi \rangle_E$ the strain orientation parameter and it can be shown that for the affine distribution:

$$\langle \sin^2 \phi \rangle_E = \frac{1}{1 + \lambda^{3/2}} \quad (4)$$

Equation (2) is based on the strain definition used in the modified series model[1]. For an isotropic sample, $\langle \sin^2 \phi \rangle_E$ equals 0.5. Usually the orientation parameter of a fibre is determined from the birefringence:

$$\langle \sin^2 \phi \rangle_{\Delta n} = \frac{2}{3}\left(1 - \frac{\Delta n}{\Delta n_{\max}}\right) \quad (5)$$

where, according to the common definition, $\langle \sin^2 \phi \rangle_{\Delta n}$ is given by:

$$\langle \sin^2 \phi \rangle_{\Delta n} = \frac{\int_0^{\pi/2} \rho(\phi) \sin^3 \phi \, d\phi}{\int_0^{\pi/2} \rho(\phi) \sin \phi \, d\phi} \quad (6)$$

and its value for the isotropic sample is 2/3. *Figure 4* shows a plot of $\langle \sin^2 \phi \rangle_E$ *versus* $\langle \sin^2 \phi \rangle_{\Delta n}$ for the Gaussian and the affine orientation distributions.

*Figure 5* depicts the stresses acting on the domain in the fibre. They are the normal stresses, $\sigma \cos^2 \phi$ and $\sigma \sin^2 \phi$ directed parallel and perpendicular to the symmetry axis, and the four shear stresses, $\tau = \sigma \sin \phi \cos \phi$. The normal stress $\sigma \cos^2 \phi$ causes extension of the domain along the chain direction, while the shear stresses bring about the rotation of the chain axes through shear deformation of the domain. The effect of the relatively small stress $\sigma \sin^2 \phi$ on the tensile deformation is not taken into consideration here. Because in linearly extended polymers the chain modulus $e_c$ is much larger than the shear modulus $g$, the tensile extension of a fibre is, to a large extent, governed by the resolved shear stress $\tau$.

As shown in *Figure 6*, the yield strain is almost independent of the strain rate, which means that yielding is caused by an immediate and permanent or plastic deformation. A shear yield stress, $\tau_y$, is proposed, above which the resolved shear stress causes a plastic rotation of the chain axes in addition to the elastic and viscoelastic rotational contributions to the fibre strain. This assumption resembles Schmid's law stating that slip begins on a given system when the shear stress resolved on that system reaches a critical value[9,10]. Thus the onset of yielding occurs when for increasing stress, $\sigma$, the shear

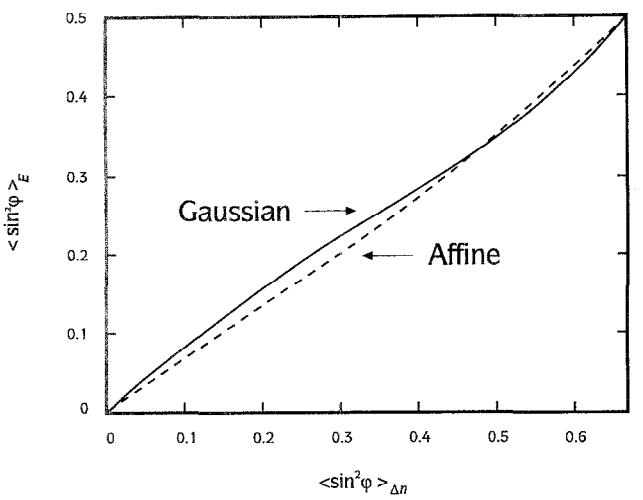


**Figure 4** The orientation parameter $\langle \sin^2 \phi \rangle_E$ *versus* the parameter $\langle \sin^2 \phi \rangle_{\Delta n}$ for the Gaussian and affine distributions

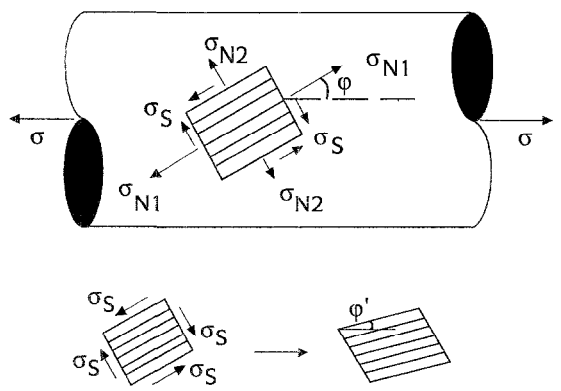


**Figure 5** The normal ($\sigma_{N1} = \sigma \cos^2 \phi$ and $\sigma_{N2} = \sigma \sin^2 \phi$) and shear stresses ($\sigma_S = \sigma \sin \phi \cos \phi$) acting on a domain with orientation angle $\phi$ with the fibre axis

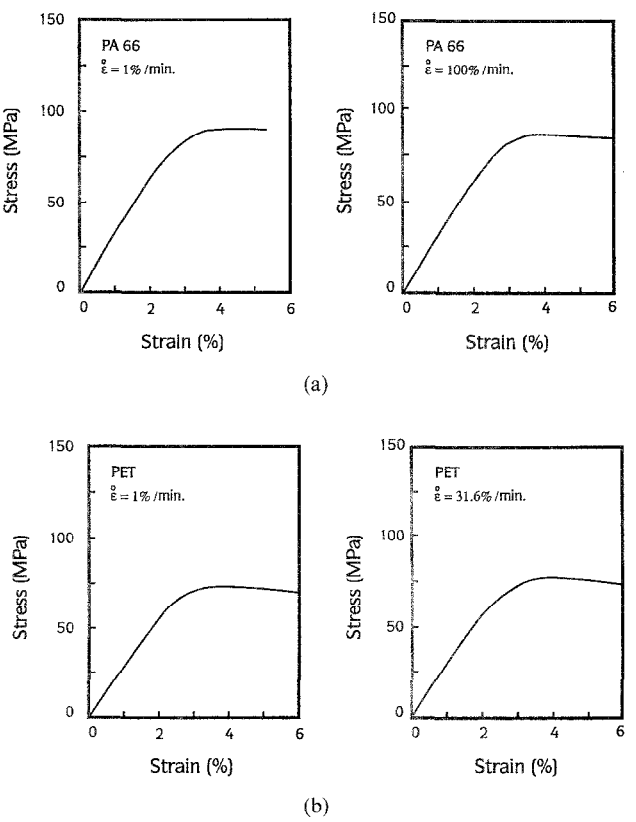


**Figure 6** The initial part of the tensile curves of isotropic sheets of (a) PA 66 and (b) PET, for different strain rates. Test length 50 mm, ISO-1 shaped samples

stresses, $\tau$, on a domain equal the critical shear stress:

$$\sigma \sin\phi \cos\phi = \tau_y \tag{7}$$

From equation (7) it follows that the plastic rotation, and consequently the plastic extension of the fibre, is initiated in domains with orientation angles (up to $\pi/4$) in the tail of the distribution $N(\phi)$. So for a broad distribution, the minimum fibre stress at which yielding starts is given by $\sigma = 2\tau_y$. A distinct effect of the plastic rotation, manifested by a drop of the slope in the tensile curve, will be observed when at least a considerable fraction of chains is subjected to a shear stress $\tau \geq \tau_y$.

In order to simplify the analysis without losing the typical features of the proposed theory, the fibril is now regarded as consisting of a bundle of parallel chains with a single orientation angle $\phi_a$, which is an average of the distribution $N(\phi)$ over the range $0 < \phi < \pi/2$ and is defined as:

$$\phi_a = \arcsin\sqrt{\langle \sin^2 \phi_0 \rangle_E} \tag{8}$$

Furthermore, we assume that the change of the orientation distribution in the initial part of the tensile curve up to $\epsilon_y$ is negligible, i.e. $\sigma = E\epsilon$, where $E$ is constant in this strain range. This leads to an approximate value for the yield strain:

$$\epsilon_y \approx \frac{\tau_y}{E \sin\phi_a \cos\phi_a} \tag{9}$$

Let $\tau_y$ be equal to $fg$, i.e. the shear yield stress is assumed to be equal to a small but constant fraction, $f$, of the shear modulus. From equations (2) and (9) it follows that:

$$\epsilon_y \approx \left(\frac{1}{e_c} + \frac{\langle \sin^2 \phi_0 \rangle_E}{2g}\right) \frac{fg}{\sin\phi_a \cos\phi_a} \tag{10}$$

It should be noted that equation (10) is only an approximation, as the precise course of the yielding in the tensile curve is controlled by the distribution $N(\phi)$. Because $e_c \gg g$ it follows from the relative derivatives

$$\begin{aligned} \frac{1}{\epsilon_y}\frac{\delta\epsilon_y}{\delta e_c} &= \frac{-2g}{2ge_c + e_c^2\langle \sin^2 \phi_0 \rangle_E} \\ \frac{1}{\epsilon_y}\frac{\delta\epsilon_y}{\delta g} &= \frac{2}{2g + e_c\langle \sin^2 \phi_0 \rangle_E} \end{aligned} \tag{11}$$

that, except for very highly oriented fibres, the yield strain is practically independent of the value of $e_c$ and depends little on $g$.

For fibres with medium and low orientation:

$$\frac{\langle \sin^2 \phi_0 \rangle_E}{2g} \gg \frac{1}{e_c} \tag{12}$$

and equation (10) can be approximated by:

$$\epsilon_y \approx \frac{f}{2} \tan\phi_a \tag{13}$$

For isotropic samples $\langle \sin^2 \phi \rangle_E = 0.5$ and because yielding in these samples will begin in the domains with an angle $\phi = \pi/4$, equation (10) reduces to:

$$\epsilon_y \approx \tfrac{1}{2} f \tag{14}$$

Because the interchain forces in the linear polymers considered here consist only of secondary interactions, such as van der Waals, dipole–dipole and hydrogen bonding, we assume that $f$ has approximately the same value in these polymers. According to equations (13) and (14) this means that the yield strain of fibres with low orientation and isotropic samples should be practically the same for these polymers.

The theory presented can also be applied to calculate the compressive yield strain of a fibre with a finite width for the chain orientation distribution and for isotropic samples. As a polymer material under compression becomes unstable above the yield stress, this stress can be considered as the compressive strength of the fibre.

## RESULTS AND DISCUSSION

Equation (14) permits the determination of the value of the parameter $f$ from the observed yield strain of isotropic samples. *Figure 6* shows the first part of the tensile curves for isotropic sheets of PA 66 and PET. An increase of the strain rate from 1 to 100% $min^{-1}$ does not change the curves significantly. The onset of yielding is observed between 2.0 and 2.5% strain, which means that $f$ is about 0.04 to 0.05. Seitz found, for a large number of isotropic polymers, that the tensile yield stress is about 2.5% of the modulus, which implies a yield strain of 2.5% and indicates that $f = 0.05$ (ref. 11). Using equation (10), the yield strain $\epsilon_y$ is now computed as a function of the strain orientation parameter $\langle \sin^2 \phi_0 \rangle_E$ for different kinds of polymer fibres. Shear moduli $g$ were derived from initial moduli $E$ using equation (2). The value of $\langle \sin^2 \phi_0 \rangle_E$ needed in this equation was calculated from $\langle \sin^2 \phi_0 \rangle_{\Delta n}$ obtained from birefringence measurements employing an affine distribution ($A$) for the PA 66, PET and the low- and medium-modulus cellulose fibres, and a Gaussian distribution ($G$) for the high-modulus cellulose fibre. The chain moduli $e_c$ for these polymers are: for PA 66, 196 GPa (ref. 12); for PET, 125 GPa (refs 13–15); and for cellulose II, 89 GPa (ref. 16). For the three PpPTA fibres, the strain orientation parameter was calculated directly from the observed azimuthal X-ray diffraction profile of the 200 reflection; subsequently, on the basis of equation (2), a linear regression was applied to the compliances and orientation parameters of these fibres yielding $g = 1.4$ GPa and $e_c = 223$ GPa. *Table 1* lists the observed birefringence, initial modulus, yield strain, the derived strain orientation parameter $\langle \sin^2 \phi_0 \rangle_E$, the calculated shear modulus $g$ and yield strain $\epsilon_y$. *Figure 7* shows the yield strain as a function of $\langle \sin^2 \phi_0 \rangle_E$ calculated with equation (10) for the various kinds of fibres using the following $g$-values: 0.5 GPa for PA 66, 1.0 GPa for PET, 1.7 GPa for cellulose II and 1.4 GPa for PpPTA. This figure confirms the conclusion drawn from equation (10) that the yield strain depends almost solely on the orientation parameter. Comparison of the observed $\epsilon_y$ values in *Table 1* with the results of *Figure 7* shows good agreement.

So far, an average angle $\phi_a$, given by equation (8), has been used to obtain an estimate of the yield strain. However, close inspection of the tensile curve reveals that yielding starts below this value. *Figure 8* shows the derivative, $d\sigma/d\epsilon$, or the differential modulus plotted *versus* the strain for PpPTA and PET fibres. First, a decrease is noticed, which is much larger for the PET

**Table 1** Birefringences $\Delta n_{max}$ and $\Delta n_{obs}$, initial modulus $E_i$, observed yield strain $\epsilon_y$, strain orientation parameter (assumed distribution: affine A, Gaussian G), shear modulus $g$ and calculated yield strain of the various fibres and the semicrystalline sheets investigated. (The $\Delta n_{max}$ values for PET, cellulose II and PA 66 have been taken from ref. 2, ref. 14 and ref. 25, respectively)

| Sample | $\Delta n_{max}$ | $\Delta n_{obs}$ | $E_i$ (GPa) | $\epsilon_y$ (obs) (%) | $\langle \sin^2 \phi_0 \rangle_E$ | $g$ (GPa) | $\epsilon_y$ (calc) (%) |
|---|---|---|---|---|---|---|---|
| PA66 | 0.082 | | | | | | |
| isotropic sheet | | | 3.7 | 2.2 | | | 2.1 |
| fibre no. 1 (as spun) | | 0.0052 | 1.6 | 1.5 | 0.46 (A) | 0.3 | 1.7 |
| fibre no. 2 | | 0.0575 | 4.4 | 0.9 | 0.132 (A) | 0.3 | 0.8 |
| PET | 0.24 | | | | | | |
| isotropic sheet | | | 3.3 | 2.2 | | | 2.2 |
| fibre no. 1 (as spun) | | 0.0853 | 5.6 | 1.7 | 0.299 (A) | 0.9 | 1.5 |
| fibre no. 2 | | 0.1803 | 13.5 | 0.5 | 0.109 (A) | 0.8 | 0.8 |
| fibre no. 3 | | 0.1806 | 16.6 | 0.5 | 0.109 (A) | 1.0 | 0.7 |
| Cellulose II | 0.054 | | | | | | |
| fibre no. 1 | | 0.026 | 11.6 | 0.9 | 0.235 (A) | 1.6 | 1.2 |
| fibre no. 2 | | 0.038 | 20.9 | 0.8 | 0.131 (A) | 1.8 | 0.9 |
| fibre no. 3 | | 0.050 | 39.9 | 0.6 | 0.048 (G) | 1.7 | 0.8 |
| PpPTA | | | | | | | |
| fibre no. 1 | | | 69 | 0.8 | 0.0274 | 1.4 | 0.55 |
| fibre no. 2 | | | 90 | 0.7 | 0.0204 | 1.4 | 0.5 |
| fibre no. 3 | | | 123 | 0.7 | 0.0097 | 1.4 | 0.5 |

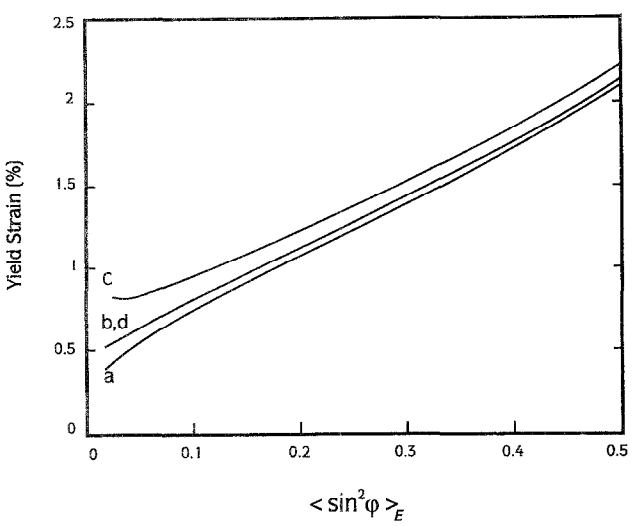


**Figure 7** Yield strain as a function of $\langle \sin^2 \phi_0 \rangle_E$ computed with equation (10) and $f = 0.04$ for (a) PA 66, (b) PET, (c) cellulose II and (d) PpPTA fibres

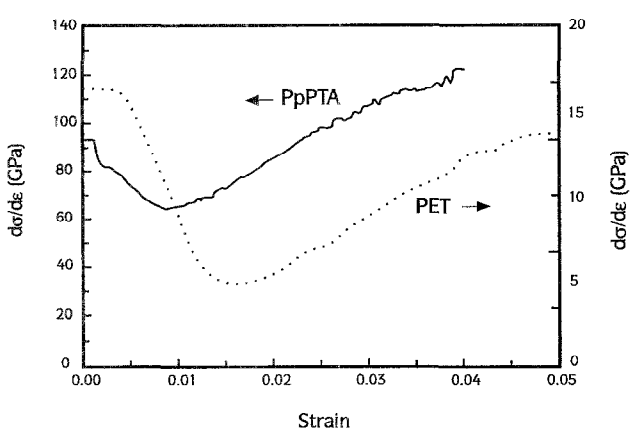


**Figure 8** The slope $d\sigma/d\epsilon$ of the tensile curves of PET and PpPTA fibres *versus* the strain

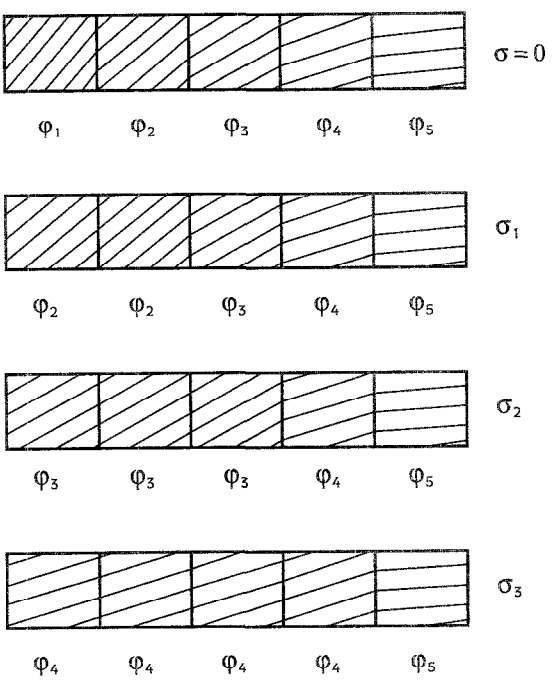


**Figure 9** Schematic representation of the yielding process in a fibril due to sequential orientation for increasing stress $\sigma$. For each domain, yielding occurs when $\sigma \sin \phi_i \cos \phi_i \geq \tau_\theta$

than for the PpPTA fibre; next, a minimum is found, usually associated with the yield; and subsequently an increase of $d\sigma/d\epsilon$ is observed. This observation can be explained by the combination of the sequential orientation mechanism and the proposed yielding of the domains in a fibril, as shown schematically in *Figure 9*. The sequential orientation is intrinsically linked to a serial arrangement of domains in the fibril of which the symmetry axes follow an orientation distribution. *Figure 3* shows a Gaussian and an affine distribution $\rho(\phi)$ with the same strain orientation parameter, $\langle \sin^2 \phi \rangle_E = 0.1472$, together with the function $N(\phi)$ being proportional to the fraction of chains at an angle $\phi$ for an

axially symmetric distribution. It shows that the affine distribution has about the same fraction of domains in the range $30° < \phi < 60°$ as the Gaussian distribution. At a stress $\sigma = 2\tau_y$, these domains are the first ones for which rotation by shear includes a plastic contribution. As the fibre stress $\sigma$ increases, more domains at smaller angles become involved in the orientation process. This means that plastic rotation actually starts at a smaller strain than calculated by equation (10). Presumably the effect of the plastic contribution on the differential modulus will be strongest near the maximum of $N(\phi)$, which accounts for the minimum in the curve of $d\sigma/d\epsilon$ *versus* the strain. A further stress increase results in an increase of the differential modulus caused by the effect of the contraction of the distribution on the modulus, which apparently exceeds the effect of the yielding process.

In semicrystalline fibres such as PET, there is usually a highly oriented crystalline phase and a much more broadly oriented amorphous phase[17–19]. Hence, the actual overall chain distribution can only be approximated by an affine distribution, and the function $N(\phi)$ will be dominated by the orientation distribution of the amorphous phase. As a result, the value for $g$ derived for the semicrystalline fibres refers to the amorphous phase. This example demonstrates that in the first part of the tensile curve for $\sigma > 2\tau_y$, the slope should progressively decrease as a result of the sequential orientation process of the oriented amorphous domains. Owing to the considerably broader distribution in PET, the decrease of the slope is likely to be relatively steeper for the PET than for the PpPTA fibres.

We are now able to provide an explanation for the difference between the first loading curve and the repeated loading or hysteresis curves, which is commonly observed for all polymer fibres considered here. In *Figure 10*, the first loading curve of a fibre is represented by section 1 and, if the strain were increased further, it would continue beyond P practically along section 4. During unloading of the fibre which has been subjected to a stress $\sigma_P$, well above the yield stress $\sigma_y$, section 3 is followed. The path followed during repeated or cyclic loading up to a stress $\sigma_P$ consists of the sections 4–3–4–3.... When the load is subsequently increased for the first time to a stress $\sigma > \sigma_P$, then from P onwards

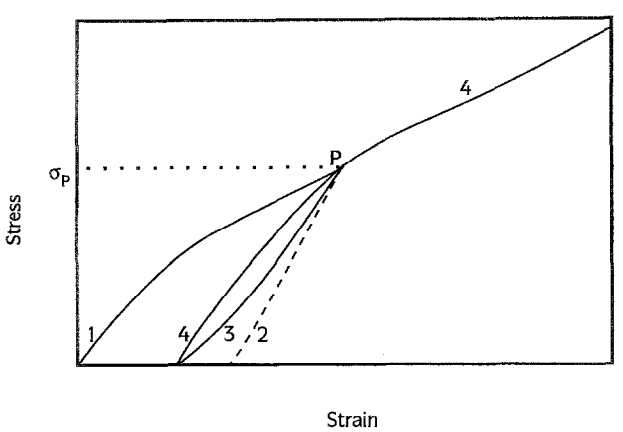


**Figure 10** Schematic representation of the tensile curves of a fibre during first loading (1), hypothetical elastic unloading (2), hysteresis (3) and (4) for a maximum stress $\sigma_P$ and subsequent continued loading (4)

section 4 is followed, which is very close to the first loading curve and involves a considerable change of slope at P. This complicated tensile behaviour can be understood on the basis of the series model and the proposed yielding mechanism, as illustrated in *Figure 9*. For small strains, the fibre response is practically elastic and, as discussed before, the yielding is caused by the onset of plastic rotation of chains, presumably by the temporary loosening or disruption of the interchain secondary bonds. The chain rotation is brought about by the resolved shear stress $\tau$ (equal to $\sigma \sin\phi \cos\phi$) which varies from domain to domain in the fibril due to the variation of the orientation angle $\phi$. Maximum shear stress is found in domains with chains having the largest orientation angle $\phi$ (angle $\phi_1$ in *Figure 9*). Hence, during the first loading of the fibre (section 1) up to a stress $\sigma_P$, the chains with angles in the range $\pi/4 < \phi < \phi_P$ undergo a plastic rotation down to an angle $\phi_P$, which according to equation (7) is given by $\phi_P = \frac{1}{2}\arcsin(2\tau_y/\sigma_P)$. If cyclic loading is now applied up to a maximum stress $\sigma_P$, no plastic rotation can occur because the chains with angles $\phi \geq \phi_P$, which allow a shear stress $\tau \geq \tau_y$, are absent. Owing to the permanent contraction of the orientation distribution caused by the first loading and the absence of plastic rotation, the upward branch (section 4) of the hysteresis curve is steeper than the first loading section (1). However, when, after a loading cycle, the stress attains for the first time a value above $\sigma_P$, domains with an orientation angle smaller than $\phi_P$ will be subjected to the shear yield stress. Accordingly, the chain rotation again contains a plastic contribution and as a result the tensile curve resumes the course followed during first loading, which is practically that of section 4 beyond P.

So far, it has been assumed that the yielding phenomenon is solely caused by plastic shearing of chains as a result of a disruption of secondary interchain bonds. However, the following observations show that yielding involves time-dependent effects as well. Firstly, the downward branch of the hysteresis cycle (section 3) clearly shows relaxation effects. If the rotation of the chains were only due to elastic and plastic shearing, then the elastic and thus steeper section 2 would have been followed during unloading of the fibre. Secondly, for increasing unloading times between repeated loading of the fibre, the reappearance of the yield in the upward branch (section 4) of the second loading cycle, as shown for PET and cellulose II fibres in *Figures 11* and *12*, is evidence of the reformation of the secondary bonds between the chains. After a waiting time of 10 min the upward branch (section 4) clearly shows yielding behaviour, which becomes more pronounced after a waiting time of 17 h. Note that the difference between the slope of section 4 before P and that beyond P decreases for increasing waiting time. When, during a loading cycle, the stress on the fibre returns to zero, the chains tend to regain their original configuration. The relaxation times depend on the flexibility of the chain and the intermolecular secondary bonding. Simultaneously with this relaxation process, secondary bonds, which were loosened during first loading, are reformed. For longer waiting times, the number of reformed secondary bonds increases, and for very long times the yielding behaviour during second loading closely resembles the yielding of the undeformed fibre.

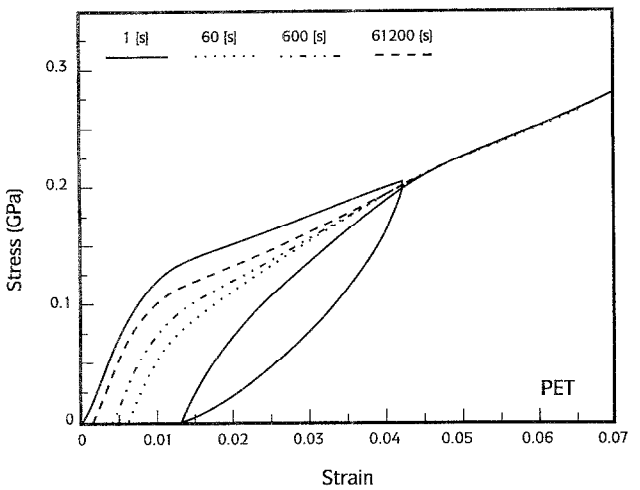


**Figure 11** First loading tensile curve and hysteresis curves of a PET fibre showing the reappearance of the yield after unloading times of 60, 600 and 61 200 s. Test length 100 mm, strain rate 25% $min^{-1}$

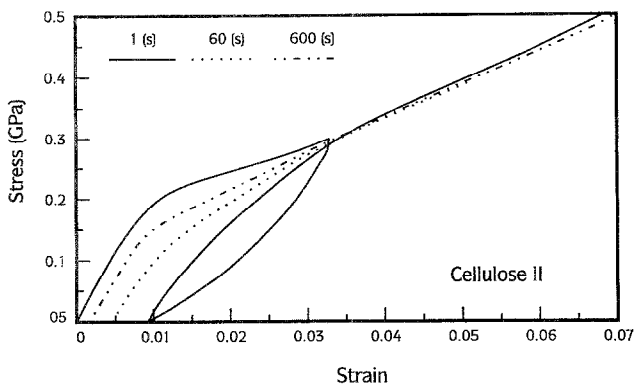


**Figure 12** First loading tensile curve and hysteresis curves of a cellulose II fibre showing the reappearance of the yield after unloading times of 60 and 600 s. Test length 100 mm, strain rate 25% $min^{-1}$

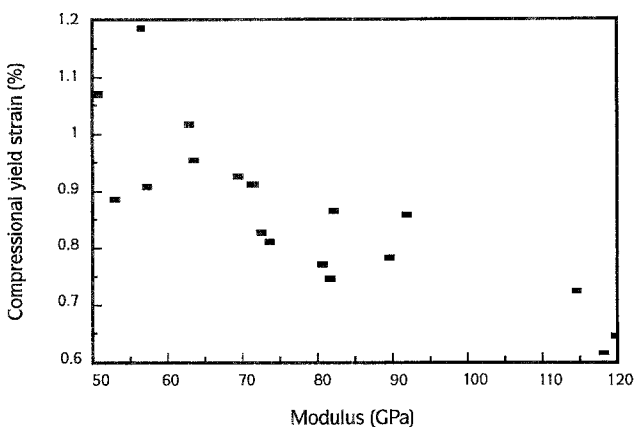


**Figure 13** Compressional yield strain as a function of the tensile modulus measured for various PpPTA fibres

The derivation presented for the yield strain in tension can also be applied to the description of yielding in axial compression, implying that the compressional yield strain, $\epsilon_{yc}$, is equal to the yield strain in tension. Depending on the definition of the yield strain $\epsilon_{yc}$ in the compression curve of isotropic specimens lies between 2 and 3% according to equation (14), which is in good agreement with the values for a variety of polymers calculated from the observed compressional yield stress and the observed compressional modulus: PET 2.6%, PBT 3.0%, polycarbonate 2.7%, PA 11 2% (ref. 20). For oriented fibres, the compressional yield strain as a function of the orientation should follow the same course as the yield strain in tension given by equation (10). Indeed, as reported by Galiotis and Vlattas[21,22], the compressional yield strain of PpPTA fibres decreases for increasing tensile modulus: $E = 70$ GPa, $\epsilon_{yc} = 0.75\%$; $E = 110$ GPa, $\epsilon_{yc} = 0.55\%$; and $E = 140$ GPa, $\epsilon_{yc} = 0.30\%$. Similar results for PpPTA fibres have been observed by van der Zwaag and Kampschoer[23]. *Figure 13* shows the results of Schaap[24] for a wide-modulus range of PpPTA fibres. For very highly oriented fibres or very small values of $\langle \sin^2 \phi_0 \rangle$, equation (10) does not apply and the axial compressional instability of these fibres may be determined by the Euler buckling mode.

In conclusion, this analysis has provided an equation for the yield strain of polymer fibres in tension and in compression, which is well confirmed by observations. Together with the results presented in refs 1, 2 and 3, this study clearly demonstrates that the resolved shear stress governs the tensile and the compressional deformation of the fibre, and that the initial orientation distribution of the chains is the most important structural characteristic determining the tensile extension of polymer fibres below the glass transition temperature, irrespective of the kind of morphology, i.e. whether the fibre is semicrystalline, like PA 66 and PET fibres, or wholly paracrystalline, like cellulose II and PpPTA fibres.

## ACKNOWLEDGEMENT

The authors wish to thank P. H. G. M. van Blokland for performing the birefringence measurements, and A. A. Schaap for giving permission to publish his compression measurements on PpPTA fibres.

## REFERENCES

1 Northolt, M. G. and van der Hout, R. *Polymer* 1985, **26**, 230
2 Northolt, M. G., Roos, A. and Kampschreur, J. H. *J. Polym. Sci. Phys. Edn* 1989, **27**, 1107
3 Northolt, M. G. and Sikkema, D. J. *Adv. Polym. Sci.* 1990, **98**, 115
4 Kuhn, W. and Grün, F. *Kolloid Zeitschr.* 1942, **101**, 248
5 Hermans, P. H. 'Physics and Chemistry of Cellulose Fibres', Elsevier, Amsterdam, 1949
6 Ward, I. M. *Br. J. Appl. Phys.* 1967, **18**, 1165
7 Picken, S. J., van der Zwaag, S. and Northolt, M. G. *Polymer* 1992, **33**, 2998
8 Northolt, M. G. and Baltussen, J. J. M. 'Proceedings of the 9th International Conference on Deformation, Yield and Fracture of Polymers, Cambridge', Institute of Materials, London, 1994
9 Cottrell, A. H. 'Dislocations and Plastic Flow in Crystals', Clarendon Press, Oxford, 1953
10 Ward, I. M. 'Mechanical Properties of Solid Polymers', Wiley-Interscience, New York, 1971
11 Seitz, T. *J. Appl. Polym. Sci.* 1993, **49**, 1331
12 Treloar, L. R. G. *Polymer* 1960, **1**, 95
13 Treloar, L. R. G. *Polymer* 1960, **1**, 279
14 Sakurada, I. and Kayi, K. *J. Polym. Sci.* 1970, **C31**, 57
15 Dulmage, W. J. and Contois, L. E. *J. Polym. Sci.* 1958, **28**, 275
16 Kroon-Batenburg, L. M. J., Kroon, J. and Northolt, M. G. *Polym. Commun.* 1986, **27**, 290
17 Heuvel, H. M. and Huisman, R. *J. Appl. Polym. Sci.* 1985, **30**, 3069
18 Huisman, R. and Heuvel, H. M. *J. Appl. Polym. Sci.* 1989, **37**, 595

19 Heuvel, H. M., Lucas, L. J., van de Heuvel, C. J. M. and de Weier, A. P. *J. Appl. Polym. Sci.* 1992, **45**, 1649
20 Agranoff, J. (Ed.) 'Modern Plastics Encyclopedia', Vol. 56, No. 10A, McGraw Hill, New York
21 Galiotis, C. and Vlattas, C. 'Proceedings of the 9th International Conference on Deformation, Yield and Fracture of Polymers, Cambridge', Institute of Materials, London, 1994
22 Vlattas, C. and Galiotis, C. *Polymer* 1994, **35**, 2335
23 van der Zwaag, S. and Kampschoer, G. in 'Intergration of Fundamental Polymer Science and Technology' Vol. 2 (Eds P. J. Lemstra and L. A. Kleintjes), Elsevier, London, 1988, p. 545
24 Schaap, A. A. Personal communication, 1994
25 Morgan, H. M. *Text. Res. J.* 1962, **32**, 866